Variable dimensionality in atoms and its effect on the ground state of the helium isoelectronic sequence

David R. Herrick and Frank H. Stillinger

Bell Laboratories, Murray Hill, New Jersey 07974

(Received 3 June 1974)

We calculate binding energies for heliumlike ions of variable dimensionality (D) with the wave functions $A = e^{(-\alpha R_1 - \beta R_2)} + e^{(-\beta R_1 - \alpha R_2)}$ and $B = A(1 + cR_{12})$. The binding energy decreases with increasing D. Functions A and B predict "critical binding dimensionalities" at $D = 3.99$ and 4.89, respectively, above which there is no binding in the hydride anion. The exact ground-state binding energy at $D = 5$ is shown to be equal to that of the doubly excited $2p^2$ $^3P^e$ state into in three dimensions. By "dimensionality scaling" of atomic units the $D = 1$ atom is transformed the δ-function model for which exact energies are known. In the infinite dimensional limit, function A predicts no exchange contribution to binding for nuclear charge $Z \geq \sqrt{2}$, with $\alpha \neq \beta$ only for $Z < \sqrt{2}$.

I. INTRODUCTION

We describe in this paper a general method for studying the ground-state binding energy of helium-like ions of arbitrary dimensionality. Dimensionality here refers to the number of Cartesian coordinates necessary to specify the position of each electron with respect to a fixed attractive nucleus located at the origin.

Variational calculations are performed to determine binding energies as a continuous function of dimensionality in order to understand better the observed energies in three dimensions. Two trial wave functions are used. The first is a simple two-parameter Hylleraas-Eckart-Chandrasehkar (HEC) function[1-3]

$$\varphi_{\text{HEC}} = e^{-\alpha R_1 - \beta R_2} + e^{-\beta R_1 - \alpha R_2}, \tag{1}$$

where R_1 and R_2 are the radial coordinates of electrons 1 and 2. The second function is the Chandrasekhar (C) modification[3] of φ_{HEC},

$$\varphi_C = \varphi_{\text{HEC}} (1 + cR_{12}), \tag{2}$$

which contains some angular correlations through the interelectron separation R_{12}. While neither of these functions represents an extremely accurate description of the exact wave function in the conventional three-dimensional ions, the novelty of our introduction of the dimensionality (D) to the problem makes them quite adequate for establishing trends in the D dependence of the binding energy over the range $1 \leq D \leq \infty$.

While the existence of D-dimensional atoms is purely hypothetical, our study of their energy is important for the following reasons. First, it is known from previous investigations of the ground state in three-dimensions by Stillinger and co-workers[4-6] that when the nuclear charge ($Z = 1/\lambda$) is sufficiently small the energy penetrates into the $1sks$ continuum corresponding to one bound and one free electron. This penetration occurs at $\lambda = 1.0975$, and as λ is increased further the energy rises until a branch-point (λ^*) singularity of order $\cong \frac{6}{5}$ is reached at $\lambda^* \cong 1.12$. Similar behavior was found[4] for the doubly excited $2p^2$ $^3P^e$ state, although the order of the singularity is $\cong 1.07$ in this state. In both cases the energy of the hydride ($\lambda = 1$) is strongly influenced by the order of the singularity due to its proximity, and a knowledge of correlation effects necessary to describe accurately the energy branch point is perforce relevant to the hydride anion at $\lambda = 1$. It is clear that the long-range correlations are most important in any state which penetrates into a continuum, and in fact a recent study by Rosenthal[7] of the δ-function atom (in which all long-range Coulomb potentials are replaced by short-range δ functions) shows that the ground-state energy is tangent to the continuum edge at $\lambda = 2.66736$. Until now, no attempt has been made to relate the λ dependence and energy branch-point behavior of these three states, since at first sight they appear to be quite independent of one another. By allowing the dimensionality of the atom to differ from $D = 3$, however, we find the remarkable result that (a) the $2p^2$ ^3P state is identical to a $1s^2$ ^1S ground state with $D = 5$, and (b) the δ-function atom ground state is identical to the limiting case of a Coulomb $1s^2$ ^1S ground state with $D = 1$. Thus by setting D at "nonphysical" values (i.e., $D \neq 3$) we are able to obtain at once a simplification and unification of seemingly unrelated questions associated with the penetration of the ground state into the continuum.

Although our application of variable dimensionality to the two-electron binding energy is the

first of its kind, there is ample evidence in other areas of physics that such a generalization is valuable. We cite for instance the theory of critical phenomena in which a branch-point singularity is observed in the free energy as temperature is varied.[8] The classical "mean-field" model predicts simple critical singularities with analytical properties the same in all numbers of dimensions. Recent work[8] has in fact shown that when $D \geq 4$ the exact critical behavior is identical to that of the classical result, and for $D < 4$ expansions of the critical exponents in power series of $(4 - D)$ have been generated.

The analogy between the critical-point behavior of the free energy and the observed singularity in the atomic ground-state binding energy at λ^* is quite interesting. For instance it can be shown[6] that any trial wave function which does not coincide with the exact wave function will give a "classical" $\frac{3}{2}$-power singularity at its λ^*. It would of course be desirable to obtain an expansion of the exact exponent in terms of D with respect to a dimensionality where the exponent is either $\frac{3}{2}$ or fixed at some precisely known value. For this reason our variational results are potentially useful, since they establish the approximate dependence of the energy upon D.

Our calculation of energies and branch-point singularities as a continuous function of dimensionality is not unlike the calculation of Regge trajectories[9,10] of poles in the S matrix as a continuous function of the angular momentum. In fact, just as discrete values of the angular momentum in Regge theory correspond to physical states, so does our discrete "spectrum" of integer dimensionalities correspond to problems of physical interest.

In Sec. II we define an extension of the one- and two-electron atomic Hamiltonians for arbitrary D, and a set of "dimensionality-scaled" length and energy units is introduced. These units show explicitly the D dependence of the Hamiltonian, and in the limit of $D=1$ the equivalence of the Coulomb potential with the δ-function model is demonstrated.

Section III contains a description of the energy expressions and integrals obtained from the HEC and Chandrasekhar wave functions. The HEC results are presented in Sec. IV, and the Chandrasekhar results are given separately in Sec. V. Discussion of these results and comparison with the "exact" energies at $D=1$, 3, and 5 appears in Sec. VI. The possibility is also raised of a "critical binding dimensionality" above which there exists no bound $1s^2$ state. Concluding remarks and a discussion of the feasibility of extending the present results to more complicated atoms and molecules appear in Sec. VII.

II. SCALED D-DIMENSIONAL HAMILTONIAN

In a D-dimensional vector space the position vector $\vec{R}$ of each electron is defined in terms of its Cartesian coordinate X_k ($k = 1, 2, \ldots, D$) with respect to a nucleus fixed at the origin. We define the D-dimensional analog of the usual ($D=3$) hydrogen atom Hamiltonian to be

$$-2H_D^0 = \Delta^{(D)} + 2/R, \tag{3}$$

with

$$(H_D^0 - E_D^0)\psi_D^0 = 0. \tag{4}$$

Here $\Delta^{(D)}$ and R are the Laplacian and the radial coordinate,

$$\Delta^{(D)} = \sum_{k=1}^{D} \frac{\partial^2}{\partial X_k^2}, \tag{5}$$

$$R = \left(\sum_{k=1}^{D} X_k^2 \right)^{1/2}. \tag{6}$$

The bound-state solutions of (4) are $\psi_D^0 = U_{n\Lambda}^{(D)}(R) Y_\Lambda^{(D)}$, where $Y_\Lambda^{(D)}$ is a D-dimensional spherical harmonic[11] with characteristic value $\Lambda(\Lambda + D - 2)$ for $\Lambda = 0, 1, \ldots$, and $U_{n\Lambda}^{(D)}$ is a radial function,

$$U_{n\Lambda}^{(D)} = NR^\Lambda e^{-kR}M(-n + \Lambda + 1; 2\Lambda + D - 1; 2kR). \tag{7}$$

Here N is a normalization factor, $k = (-2E)^{1/2}$, and M is the confluent hypergeometric function.[12] The energy is determined from integer values of the principal quantum number $n \geq \Lambda + 1$ by the relation

$$E_n^D = -\tfrac{1}{2}[n + (D-3)/2]^{-2}, \tag{8}$$

in which Λ does not appear. This degeneracy of states of different Λ having the same principal quantum number was shown by Alliluev[13] in direct analogy to Fock's[14] result for $D=3$.

Defining $\varphi_{n\Lambda}^{(D)} = R^{(D-1)/2}U_{n\Lambda}^{(D)}$, the equivalent radial Hamiltonian results:

$$\left[-\frac{\partial^2}{\partial R^2} + \frac{\Lambda(\Lambda + D - 2) + [(D-1)/2][(D-3)/2]}{R^2} \right.$$

$$\left. - \frac{2}{R} - 2E_n^D \right]\varphi_{n\Lambda}^{(D)} = 0. \tag{9}$$

This explicit dependence upon D shows that for $D > 3$ there is a repulsive R^{-2} "dimensionality barrier" which produces states more diffuse radially than those at $D=3$ having the same n and Λ.[15] For $1 < D < 3$ on the other hand the R^{-2} potential is attractive relative to $D=3$, and gives rise to more tightly bound states.

Thus, as D is increased the states tend to behave very much as excited states do when $D=3$. In fact it has been shown[16] that Eq. (9) is invariant to the transformation $(\Lambda, D, n) \to (\Lambda + 1, D - 2, n + 1)$. For instance the $1s$ ($D=5$) radial function is iden-

tical to the $2p$ ($D=3$) radial function.[17]

The corresponding two-electron Hamiltonian is

$$-2H_D = \Delta_1^{(D)} + \Delta_2^{(D)} + \frac{2}{R_1} + \frac{2}{R_2} - \frac{2\lambda}{R_{12}}, \tag{10}$$

where indices 1 and 2 label the electrons and $R_{12} = |\vec{R}_1 - \vec{R}_2|$. Our units are such that the coupling parameter $\lambda = Z^{-1}$ is continuous, with the discrete values $\lambda = 1, \frac{1}{2}, \frac{1}{3}, \ldots$ representing the H$^-$, He, Li$^+$, ... isoelectronic sequence. It is convenient at this point to introduce a new system of units with the property that when $\lambda = 0$ the ground-state energy is constant with respect to D. In this manner variations in the binding energy as a function of D at $\lambda \neq 0$ can be attributed primarily to $1/R_{12}$. In addition these units will allow us to consider the ground state at $D=1$, which we see from Eq. (8) is at negative infinity when $\lambda = 0$. We therefore define a set of "dimensionality-scaled atomic units" for the length and energy:

$$\vec{r}_K = [2/(D-1)]\vec{R}_k, \quad k=1,2 \tag{11a}$$

$$h_D = [(D-1)/2]^2 H_D, \tag{11b}$$

$$\epsilon_D = [(D-1)/2]^2 E_D. \tag{11c}$$

These relations are designed so that when $D=3$, length and energy are unchanged. When $\lambda = 0$, the ground-state energy is at -1 with respect to the doubly ionized species. The singly ionized continuum edge is at $\epsilon_D = -\frac{1}{2}$ for all λ. We do not consider values of $D<1$, since in unscaled units the $\lambda = 0$ ground state is unnormalizable.

In general, the ground-state wave function is dependent upon only the three coordinates r_1, r_2, and $r_{12} \equiv u$, and transformation of (10) to this system gives

$$h_D = G_0 + (D-1)G_1, \tag{12a}$$

with

$$-2G_0 = \frac{\partial^2}{\partial r_1^2} + \frac{\partial^2}{\partial r_2^2} + \frac{2\partial^2}{\partial u^2} + \frac{u^2 + r_1^2 - r_2^2}{r_1 u} \frac{\partial^2}{\partial r_1 \partial u}$$
$$+ \frac{u^2 + r_2^2 - r_1^2}{r_2 u} \frac{\partial^2}{\partial r_2 \partial u} \tag{12b}$$

and

$$-2G_1 = \frac{1}{r_1}\frac{\partial}{\partial r_1} + \frac{1}{r_2}\frac{\partial}{\partial r_2} + \frac{2}{u}\frac{\partial}{\partial u} + \frac{1}{r_1} + \frac{1}{r_2} - \frac{\lambda}{u}. \tag{12c}$$

In this form the explicit D dependence of h_D is obtained, and (12a) may be used to define a generalization of the Hamiltonian to nonintegral values of D, although only integer values of D have representations in Cartesian coordinates.

We may also choose to expand h_D about a fixed dimensionality D_0, and one obtains immediately from (12a) the relation for $D_0 > 1$:

$$h_D = h_{D_0} + (D - D_0)G_1. \tag{13}$$

In this manner the energy ϵ_D can be expressed as a zeroth-order energy ϵ_{D_0} plus a perturbation expansion in $(D - D_0)$ at each value of λ. Equation (13) differs from the usual perturbation equation in one important respect, namely, that the integration volume element in D dimensions is not equal to the volume element in D_0 dimensions.

We do not use perturbation theory in the present paper. Instead, we obtain upper bounds to the exact ground-state energy ϵ_D for each trial function φ_T by means of the usual variation theory on

$$\epsilon_D^T = \langle \varphi_T | h_D | \varphi_T \rangle / \langle \varphi_T | \varphi_T \rangle \geq \epsilon_D. \tag{14}$$

(This inequality is only valid below the continuum edge.)

In concluding this section, we note that the Coulomb potential-energy terms in Eq. (12) are of the form $(D-1)/|x|$, where $|x| = r_1$, r_2, or r_{12}. In the limit of $D \to 1$ these terms clearly vanish, except when $|x| = 0$. Because the volume element contains a factor $|x|^{D-1}$, as $D \to 1$ we may replace the Coulomb terms by $\lim_{D \to 1}(D-1)|x|^{D-2} = 2\delta(x)$. Here $\delta(x)$ is the Dirac δ function. Thus the Hamiltonian at $D=1$ becomes

$$h_1 = -\frac{1}{2}\left(\frac{\partial^2}{\partial x^2} + \frac{\partial^2}{\partial y^2}\right) - \delta(x) - \delta(y) + \lambda\delta(x - y),$$
$$-\infty \leq x, y \leq \infty \tag{15}$$

where x and y are the one-dimensional coordinates of electrons 1 and 2.

At $\lambda = 0$ the ground-state eigenfunction of (15) is $e^{-|x|-|y|}$. In dimensionality-scaled atomic units the one-electron hydrogenic energy of Eq. (8) is $\frac{1}{2}[(D-1)/(2n + D - 3)]^2$, and thus as $D \to 1$ only one bound state exists, with $n=1$. This establishes the fact that there is only one bound eigenfunction of (15).

The one-electron δ-function model for atoms and molecules has been studied by Frost.[18] Application of analytic perturbation theory to the two-electron-model atom has been made by White and Stillinger,[19] and exact energies for $\lambda > 0$ were recently reported by Rosenthal.[7] Each of these earlier investigations regarded the model as representing only qualitatively the properties of the three-dimensional Coulomb problem. We have demonstrated that they are actually solutions of the *same* Schrödinger equation differing only by continuous scaling of the dimensionality.

III. VARIATIONAL CALCULATIONS

The HEC wave function defined in Eq. (1) leads in a straightforward manner to an energy expression in terms of a scale factor α and $\eta = \beta/\alpha$,

$$\epsilon_D^{\text{HEC}} = \alpha^2[J_0/J_3] + \alpha[-J_1 + \lambda(J_2/J_3)] , \tag{16}$$

with

$$2J_0 = 2(1 + \eta^2)(1 + \eta)^{2D} + (4\eta)^{D+1} , \tag{17}$$

$$J_1 = (1 + \eta) , \tag{18}$$

$$J_2 = \eta(\eta + 1)M_D \left[(4\eta)^{D-1} + (1 + \eta)^{2D-2} \right.$$
$$\left. \times F\left(\tfrac{1}{2}, \frac{1-D}{2}; \frac{D+2}{2}; \left(\frac{1-\eta}{1+\eta}\right)^2 \right) \right] , \tag{19}$$

$$M_D = \frac{2^{D+1}\Gamma((D+1)/2)^2\Gamma(D+\tfrac{1}{2})}{\Gamma(D)\Gamma(D+1)\Gamma(\tfrac{1}{2})} , \tag{20}$$

$$J_3 = 2(1 + \eta)^{2D} + 2(4\eta)^D . \tag{21}$$

F is the hypergeometric function[12]

$$F(a, b; c; x) = 1 + \frac{ab}{c}\frac{x}{1!} + \frac{a(a+1)b(b+1)}{c(c+1)}\frac{x^2}{2!} + \cdots , \tag{22}$$

and $\Gamma(y)$ is Euler's gamma function. Since φ_{HEC} is symmetric in α and β, we need consider only values of $\eta \leq 1$ in the variation of ϵ_D^{HEC}.

Minimization with respect to the scaling parameter α leads to

$$(\epsilon_D^{\text{HEC}})_{\text{best}} \ _\alpha = -[J_1 J_3 - \lambda J_2]^2/4J_0 J_3 . \tag{23}$$

The minimization of (23) with respect to η was then done numerically. The hypergeometric series is convergent for $\eta \geq 0$, and when D is an odd integer it truncates to a simple polynomial.

The energy expression for the Chandrasekhar wave function is much more complicated than the HEC result, and we present only the necessary integrals. Generalizing to arbitrary dimensionality the Fourier-transform method used by Bonham and Kohl,[20] we write for dimensionality D

$$\frac{e^{-ar}}{r} = \frac{\Gamma(\nu + \tfrac{1}{2})}{2\Gamma(\tfrac{1}{2})\pi^{\nu+1}} \int d\vec{k} \frac{e^{-i\vec{k}\cdot\vec{r}}}{(a^2 + k^2)^{\nu+1/2}} , \tag{24}$$

with $2\nu = D - 2$. Defining

$$W_D(a, b, c) = \int d\vec{r}_1 \int d\vec{r}_2 \frac{e^{-ar_1}}{r_1} \frac{e^{-br_2}}{r_2} \frac{e^{-cr_{12}}}{r_{12}} , \tag{25}$$

integrals of the type

$$G_D^k(a, b) = \int d\vec{r}_1 \int d\vec{r}_2 \frac{e^{-ar_1}}{r_1} \frac{e^{-br_2}}{r_2} r_{12}^{k-1} \tag{26}$$

are evaluated as

$$G_D^k(a, b) = \lim_{c \to 0} \left[\left(-\frac{\partial}{\partial c}\right)^k W_D(a, b, c) \right] . \tag{27}$$

Substitution of Eq. (24) into Eq. (25) leads after considerable algebraic manipulation to the result

$$G_D^k(a, b) = N_D F\left(\frac{1-k}{2}, \frac{3-D-k}{2}; \frac{D}{2}; y\right) \frac{(a+b)^{k-1}}{(ab)^{k+D-2}} \tag{28}$$

$$= N_D F\left(\frac{k+D-1}{2}, \frac{2D+k-3}{2}; \frac{D}{2}; y\right)$$

$$\times \frac{4^{k+D-2}}{(a+b)^{2D+k-3}} , \tag{29}$$

where

$$y = \left(\frac{a-b}{a+b}\right)^2 \tag{30}$$

and

$$N_D = \frac{(4\pi)^{D-1}\Gamma(k+D-1)\Gamma((k-1)/2+D-1)\Gamma((D-1)/2)^3}{2^k\Gamma(D-1)^2\Gamma((k+D)/2)} . \tag{31}$$

In going from Eq. (28) to Eq. (29) we have used the hypergeometric identity[12]

$$F(A, B; C; Z) = (1 - Z)^{C-A-B}F(C - A, C - B; C; Z) . \tag{32}$$

Integrals of the type

$$K_D(i, j, k) = \int d\vec{r}_1 \int d\vec{r}_2 e^{-ar_1 - br_2} r_1^{i-1} r_2^{j-1} r_{12}^{k-1} \tag{33}$$

necessary for the evaluation of ϵ_d^C can then be obtained by taking appropriate derivatives, namely,

$$K_D(i, j, k) = \left(-\frac{\partial}{\partial a}\right)^i \left(-\frac{\partial}{\partial b}\right)^j G_D^k(a, b) . \tag{34}$$

In taking the derivatives with respect to a and b we have found it most convenient to use Eq. (29) for $G_D^k(a, b)$, and then to use the transformation in Eq. (32) to obtain negative hypergeometric indices whenever possible. When $D = 3$ the hypergeometric function in (28) is reducible to the algebraic function

$$G_3^k(a, b) = (4\pi)^2\Gamma(k+1)(a^2 - b^2)^{-1}(b^{-k-1} - a^{-k-1}) , \tag{35}$$

which is identical to Eq. (3) of Bonham and Kohl when their parameter $\alpha = 0$.

In optimizing the Chandrasekhar energy, minimization with respect to the scale parameter α was performed exactly, and then $\eta = \beta/\alpha$ and $\gamma = c/\alpha$ were varied by a numerical-pattern search[21] for values of $D \leq 7$. No systematic investigation of the Chandrasekhar energy for $D > 7$ was made,[22] since the λ dependence of ϵ_D^{HEC} and ϵ_D^C at $D = 7$ was nearly identical, the variationally optimized energies differing at most by only 0.008 a.u in dimensionality-scaled units.

IV. HEC NUMERICAL RESULTS

A. General features

The λ dependence of the HEC ground-state energy for $D = 1, 2, 3, 4, 7, \infty$ is illustrated in Fig. 1, and an expanded version near $\lambda = 1$ is provided in Fig. 2. These results show a marked decrease in the binding energy for $\lambda > 0$ as D increases. A detailed analysis of the $D = 3$ curve appears in a paper by Stillinger and Stillinger.[5] Figure 3 shows the corresponding dependence of η for $1 \geqslant \eta \geqslant 0$. For each finite $D > 1$, η drops smoothly from unity as λ is increased from zero until a point λ_D^* is reached where $(\partial\eta/\partial\lambda) = -\infty$. This corresponds to a branch point singularity in $\epsilon_D^{\mathrm{HEC}}$ of order $\frac{3}{2}$. The portion of the curve with $(\partial\eta/\partial\lambda) > 0$ corresponds to a maximum in the variational energy, and is of course nonphysical. The point λ_D^{**} defined by $(\partial\eta/\partial\lambda) = +\infty$ represents another singularity in the energy, and a further decrease in η with increasing λ indicates the existence of a second minimum branch of the HEC energy ending at $\lambda = 1$ with $\eta = 0$. The value $\eta = 0$ indicates an infinitely extended outer orbital, i.e., the removal of one electron to infinity at $\epsilon_D = -\frac{1}{2}$. Comparison of Figs. 1–3 shows that in general the HEC energy curves can be divided into the following two classes.

Class I: Energy less than $-\frac{1}{2}$ *at* $\lambda = 1$. In these curves (for example, $D = 3$ in Fig. 2) the HEC energy penetrates the continuum edge at $\epsilon_D = -\frac{1}{2}$ with a finite slope, and ends at the branch point λ^*. In each case the second minimum in $\epsilon_D^{\mathrm{HEC}}$ does not appear to have a physical interpretation, and has not been illustrated.

Class II: Energy greater than $-\frac{1}{2}$ *at* $\lambda = 1$. In these curves (for example, $D = 7$ in Fig. 2) the first and second HEC minimum-energy branches inter-
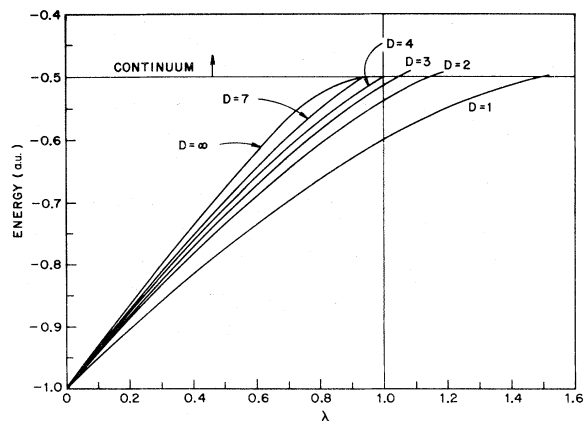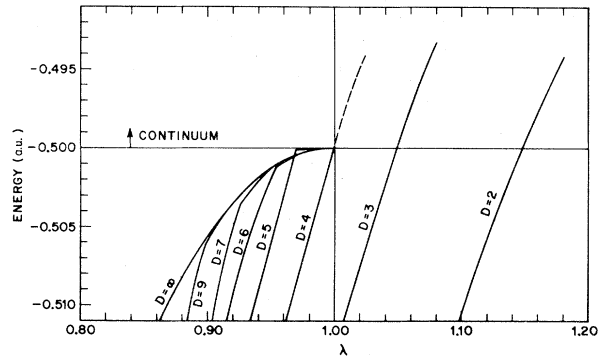

FIG. 2. Expanded version of HEC energies in Fig. 1 in the region $\lambda \cong 1$. The broken-line extension of the $D = 4$ curve represents a nonphysical energy minimum, and is included for comparison with the $D = 2, 3$ curves in which that same energy branch does represent the physical state.

sect at $\lambda \equiv \lambda_i < 1$. Thus in the interval $0 \leqslant \lambda \leqslant \lambda_i$ the first minimum branch (larger η) of $\epsilon_D^{\mathrm{HEC}}$ represents the lowest HEC upper bound to the exact energy. In the interval $\lambda_i \leqslant \lambda \leqslant 1$, however, it is the *second* minimum branch (smaller η) which represents the lowest HEC upper bound to the exact ϵ_D.

The lowest-energy HEC state for these class-II curves therefore has a discontinuous first derivative with respect to λ, and a discontinuity in η at $\lambda = \lambda_i$. This is of course an artifact of the HEC approximation, since it has been proven by Kato[23] that an isolated energy eigenvalue is an analytic function of λ. The HEC energy for $D = 7$ on the region of λ_i is illustrated separately in Fig. 4, with each portion of the curve explicitly labeled. The qualitative features of each class-II curve near λ_i are identical to the $D = 7$ result, except that the triangular region moves entirely below $\epsilon = -\frac{1}{2}$ as D increases.
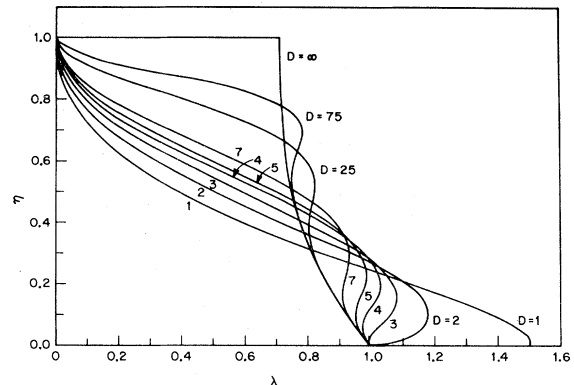

FIG. 1. λ dependence of HEC variational ground-state energies for heliumlike ions of variable dimensionality D. λ is the coupling parameter in Eq. (10).

FIG. 3. λ dependence of the optimized HEC parameter $\eta = \beta/\alpha$ for variable dimensionality, where α, β are the orbital exponents of Eq. (1).

From our definitions of class-I and class-II energy curves it is clear in the HEC approximation that a unique "critical binding dimensionality" (D_c) exists such that at $\lambda = 1$, $\epsilon_{D_c}^{HEC} = -\frac{1}{2}$, but $\epsilon_D^{HEC} < -\frac{1}{2}$ for all $D < D_c$. The HEC value is $D_c \cong 3.99$. For $D > D_c$ there is no binding at $\lambda = 1$, and only continuum states for $\lambda > 1$. The limiting case $D = 1$ and $D = \infty$ are particularly interesting because the minimization of ϵ_D^{HEC} can be accomplished analytically, as we now show.

B. Results for $D = \infty$

From Eq. (6) we obtain in the limit $D \to \infty$

$$-2\epsilon_\infty^{HEC} = [1 + \eta - \lambda\eta(1 + \eta^2)^{-1/2}]^2(1 + \eta^2)^{-1}. \qquad (36)$$

Minimization of ϵ_∞^{HEC} with respect to η gives rise to only two energy minima on the interval $0 \leqslant \eta, \lambda \leqslant 1$, designated A and B in what follows. The first (A) is

$$\eta_A = 1, \qquad (37a)$$

$$\epsilon_\infty^A = -[1 - (\lambda\tfrac{1}{4}\sqrt{2})]^2, \qquad (37b)$$

corresponding to a screened hydrogenic wave function. ϵ_∞^A is a minimum only when $0 \leqslant \lambda \leqslant 1/\sqrt{2}$, while for larger λ it becomes a maximum. The second energy branch (B) is
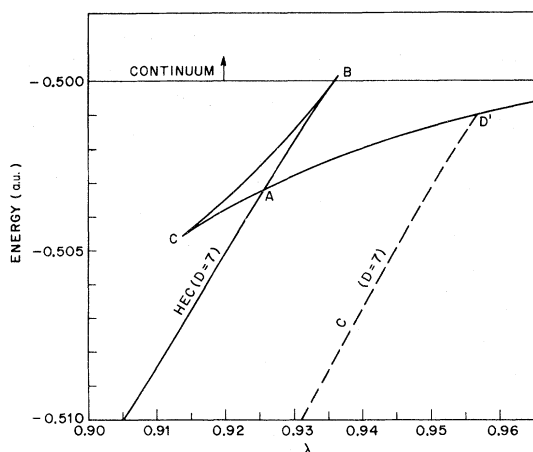

FIG. 4. λ dependence of HEC and Chandrasekhar (C) energies for dimensionality $D = 7$, illustrating the two physical minimum-energy branches discussed in the text. Segment BC represents an energy maximum, while CA and AB represent nonphysical energy minima. Point A (at λ_i) defines the intersection of the two minimum branches. For $\lambda > \lambda_i$ the second minimum branch approaches the continuum edge tangentially at $\lambda = 1$. The intersection of the two Chandrasekhar minimum-energy branches occurs at D'. For higher values of λ the Chandrasekhar and HEC energies are indistinguishable on this graph.

$$\eta_B = [\lambda^2 - (2\lambda^2 - 1)^{1/2}](1 - \lambda^2)^{-1}, \qquad (38a)$$

$$\epsilon_\infty^B = -(\lambda^2 + 1)^2(8\lambda^2)^{-1}, \qquad (38b)$$

and represents the energy minimum only for $\lambda \geqslant 1/\sqrt{2}$. Thus at $D = \infty$ the two HEC energy branches are joined at $\lambda_i = 1/\sqrt{2}$ and it is easily seen that $\partial\epsilon_\infty^{HEC}/\partial\lambda$ and η are continuous at λ_i in contrast to the discontinuities observed at lower finite D.

The most interesting feature of the $D = \infty$ state is that exchange correlation, which is described in the HEC function by a value of $\eta \neq 1$, does not contribute to stability of the ground state for $\lambda < 1/\sqrt{2}$. For $\lambda > 1/\sqrt{2}$, η decreases rapidly to zero at $\lambda = 1$. Thus in the HEC approximation the electrons move independently of each other when $\lambda < 1/\sqrt{2}$. At $\lambda = 1/\sqrt{2}$ a radial instability occurs which allows the electrons to take advantage of radial correlation. One electron becomes rapidly more diffuse as λ increases until at $\lambda = 1$ it becomes ionized.

C. HEC results for $D = 1$

In this case minimization of ϵ_1^{HEC} with respect to η leads to the condition that

$$(2\lambda - 3)(1 + \eta^6) + (14\lambda - 22)(\eta + \eta^5)$$
$$+ (38\lambda - 3)(\eta^2 + \eta^4) + (20\lambda + 76)\eta^3 = 0. \qquad (39)$$

At $\eta = 0$ we see that $\lambda = \frac{3}{2}$, in contrast to $D > 1$, where $\eta = 0$ at $\lambda = 1$. Equation (39) is transformed into a cubic equation by the substitution $z = 2\eta(1 + \eta^2)^{-1}$ to give

$$(2\lambda - 3) + (7\lambda - 11)z + (8\lambda - 1)z^2 + (-\lambda + 15)z^3 = 0, \qquad (40)$$

for which exact solutions are known.[12] The branch-point singularity occurs at $\lambda^* = 1.50256869$, with $\epsilon_1^{HEC} = -0.49998246$, so that the energy has just barely penetrated into the continuum. In terms of z the energy is

$$\epsilon_1^{HEC} = -\frac{[1 + z][1 + (3 - \lambda)z]^2}{2[1 + 3z][1 + z + 2z^2]}, \qquad (41a)$$

$$z = 2\eta(1 + \eta^2)^{-1}. \qquad (41b)$$

The explicit form of the HEC energy minimum as a function of λ is complicated, and we omit detailed discussion at present. In spite of the complexity, however, it represents the simplest example of an analytic variational energy for the Coulomb potential which penetrates into the continuum.

V. CHANDRASEKHAR NUMERICAL RESULTS

Qualitatively the Chandrasekhar energy curves are similar to the HEC results, as shown in Fig. 5 for $D = 1$, 1.1, 2, 3, 4, 5, and 7. It is not surprising that the inclusion of angular correlation in
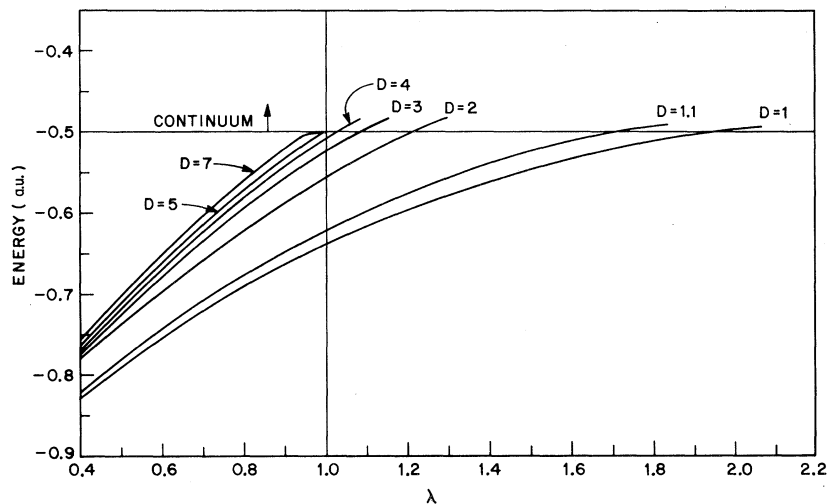
FIG. 5. λ dependence of Chandrasekhar variational energies for variable dimensionality D.

the Chandrasekhar wave function leads to an increase in stability with respect to the HEC results, but at the higher values of D this difference is minimal. Two important improvements over the HEC results are that (i) the critical binding dimensionally above which the $\lambda = 1$ ion ceases to be bound is now at $D_c \cong 4.89$ compared with the HEC value 3.99, and (ii) at $D = 1$ the increased stability has pushed λ^* out to 2.06.

At $D = 3$ the Chandrasekhar results are very similar to those reported by Stillinger and Weber[6] for the Bonham-Kohl (BK) function[20]

$$\varphi_{BK} = \varphi_{HEC}(1 + Ke^{-kr_{12}}), \qquad (42)$$

as indicated by the fact that k is generally small ($\cong 0.1$). The Chandrasekhar branch-point singularity occurs at $\lambda^* = 1.1504$, in comparison with $\lambda^* = 1.1517$ for the BK function.

Typical values of the Chandrasekhar parameters γ and η are shown in Figs. 6 and 7 for the mini-

mum-energy branches only. Note the extremely rapid rise of γ for the larger D values, indicating a much stronger angular correlation than is seen at $D = 3$. For $D < 3$ the angular correlation is slightly larger than at $D = 3$. The corresponding η vs λ curves are similar to those of the HEC function, although tending to be slightly larger for given D.

In the region near $\lambda = 1$ the second minimum-energy branch is nearly identical to that of the HEC energy for $D > 5$. This is illustrated in Fig 4 at $D = 7$. The point D' represents the intersection at λ_1 of two minimum-energy branches. For $\lambda > \lambda_i$ the Chandrasekhar energy is indistinguishable from the HEC result. The energy in this region is approximated quite well by Eq. (38b) for the infinite-dimensional HEC energy, owing to the extreme diffuseness of the wave function.
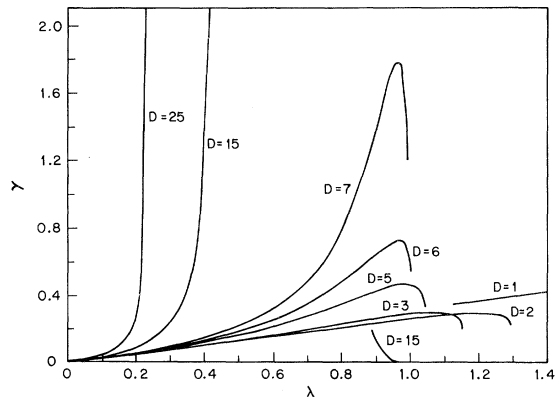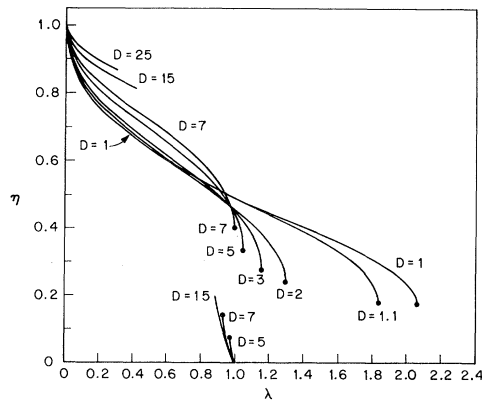

FIG. 6. λ dependence of the optimized Chandrasekhar parameter $\gamma = c/\alpha$ for variable dimensionality, with α and c defined in Eq. (2).

FIG. 7. λ dependence of Chandrasekhar parameter $\eta = \beta/\alpha$ for variable dimensionality, with α and β defined in Eq. (2). Filled circles indicate vertical tangencies associated with the branch-point behavior of the energy.

VI. RATIONALE FOR EFFECT OF D ON BINDING

A. Importance of the volume element

It is evident from the results presented in Secs. IV and V that there is a tendency for the ground-state binding energy to decrease with increasing dimensionality. At first sight this observation appears to be in direct contradiction with naive intuition, which suggests that as the number of Cartesian coordinates (D) increases the electrons will be able to avoid each other more easily than they can in lower dimensionalities.

The key to understanding the binding trend at higher D lies in the observation we made in Sec. II, that ground states for $D > 3$ behave like doubly excited states at $D = 3$. The reason for this was that the volume element, which is proportional to $(r_1 r_2)^{D-1}$, keeps both electrons far from the nucleus. The electrons are thus screened from the nucleus by an effective "dimensionality barrier." This results in a reduction of the nuclear attraction energy, and also an increase in the average repulsion energy between the electrons.

The latter point is illustrated by the following example. Consider the "radial limit" of the Coulomb interaction, defined by

$$V_D = \frac{\int d\Omega_1 \int d\Omega_2 (1/r_{12})}{\int d\Omega_1 \int d\Omega_2} , \qquad (43)$$

where the integrations are performed only over the angular coordinates of electrons 1 and 2. Straightforward integration gives the general result as a continuous function of D that

$$V_D = (1/r_>) F\left(\tfrac{1}{2}, \frac{3-D}{2}; \frac{D}{2}; \left(\frac{r_<}{r_>}\right)^2\right), \qquad (44)$$

with $r_>$ and $r_<$, respectively, the larger or smaller values of r_1 and r_2, and F is the hypergeometric function [Eq. (22)]. If we fix the value of $r_</r_>$ and increase D we see that V_R actually *decreases* in magnitude. For instance, $V_3 = 1/r_>$, $V_5 = (1/r_>)$ $\times [1 - \tfrac{1}{5}(r_</r_>)^2]$, and $V_\infty = (r_1^2 + r_2^2)^{-1/2}$. The volume element increases much more rapidly with D, however, and using the $\lambda = 0$ wave function $\varphi^0 = e^{-r_1 - r_2}$ the average repulsion energy is found to be

$$\frac{\langle \varphi^0 | r_{12}^{-1} | \varphi^0 \rangle}{\langle \varphi^0 | \varphi^0 \rangle} = \frac{\Gamma((D+1)/2)\Gamma(D+\tfrac{1}{2})}{\Gamma(D+1)\Gamma(D/2)} , \qquad (45)$$

which is of course equal to the first-order energy $(\epsilon_D^{(1)})$ in a λ-series expansion of the exact ϵ_D. Starting at $D = 1$, $\epsilon_D^{(1)}$ equals $\tfrac{1}{2}$, and then increases slowly as D ascends until the limiting value $\epsilon_D^{(1)}$ $= 1/\sqrt{2}$ is reached at $D = \infty$.

B. Comparison of variational results with "exact" results for $D = 1, 3, 5$

We prove in Appendix A that the $1s^2 {}^1S$ energy and wave function at $D = 5$ are identical (to within trivial factors) to those for the doubly excited $2p^2 {}^3P$ state at $D = 3$. This remarkable result allows us to use the accurate Pekeris[24] variational energies and the perturbation series expansions of Midtdal[25] and Aashamar[26] for the $1s^2$ and $2p^2$ states as well as the accurate δ-function-model $(D = 1)$ results of Rosenthal[7] for comparison with the HEC and Chandrasekhar results. The corresponding exact $D = 1$, 3, and 5 energy curves appear in Fig. 8. All three curves are bound at $\lambda = 1$ (class I). The ϵ_1 curve remains bound out to $\lambda = 2.66736$, at which point the energy is *tangent* to the continuum, in contrast to ϵ_3 and ϵ_5, which penetrate into the continuum with positive slope.

The nature of the exact energy curves for $D > 5$ is not known and, in particular, it is not clear whether there exists a critical bonding dimensionality for the *exact* energy as indicated by both the HEC and Chandrasekhar wave function. Figure 9 illustrates the dimensionality dependence of the ionization potential (IP $= 0.5 - \epsilon_D$) at $\lambda = 1$ for the HEC, Chandrasekhar, and exact energies. The HEC IP goes to zero with slope $\partial(\text{IP})/\partial D = -0.0102$ at $D_c^{\text{HEC}} = 3.987$, while the Chandrasekhar IP intersects with a slope $\partial(\text{IP})/\partial D = 0.0089$ at $D_c^C = 4.891$. If the exact IP curve does have a finite D_c, then its slope at $\lambda = 1$ is obtained from

$$\frac{\partial \epsilon_D}{\partial D} = \frac{\langle \varphi_D | G_1 | \varphi_D \rangle}{\langle \varphi_D | \varphi_D \rangle} , \qquad (46)$$

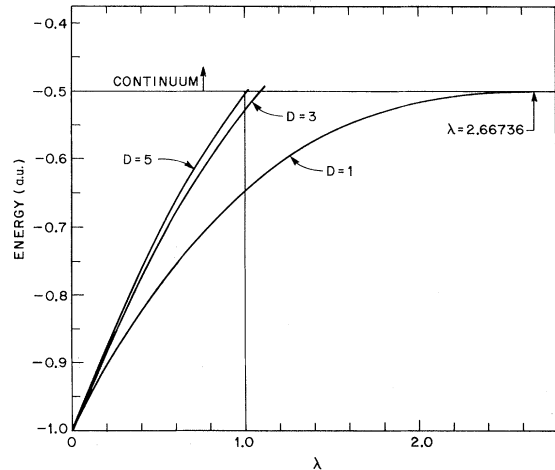where G_1 was defined in Eq. (12) and φ_D is the

FIG. 8. λ dependence of exact ground-state energy for dimensionality $D = 1$, 3, 5 as described in text.

exact wave function at $\lambda = 1$. It is evident from the slope of ϵ_D in Fig. 9 that $\partial \epsilon_D / \partial D > 0$ over the range D shown, and it is possible that the IP approaches zero tangentially. Equation (46) would support this presumption, if φ_D becomes infinitely extended as the $\lambda = 1$ IP declines to zero. The exact IP curve in Fig. 9 represents a parabolic fit in D^{-1} to the IP's at $D = 1, 3, 5$. Extrapolation of this curve to IP $= 0$ gives $D_c \cong 5.18$.

Figure 10 provides a comparison of magnitudes of λ^* for HEC, Chandrasekhar, and the exact energy curves with increasing D. When $3 \leqslant D \leqslant 5$ the value of λ^* for the exact energy is bounded by the Chandrasekhar and HEC results. For $D < 3$ the exact curve actually rises above the Chandrasekhar curve at some point, reaching a value of $\lambda^* = 2.66736$ at $D = 1$. Note that in the region $D \cong 3$ both the HEC and Chandrasekhar wave functions give a reasonable description of λ^*. As one moves to either higher or lower D, however, more subtle correlation terms must be included in the wave function.

The dependence of the branch-point critical exponent θ^* upon D is illustrated in Fig. 11. For the HEC and Chandrasekhar wave functions a constant $\frac{3}{2}$ power is found. The exact results show that θ^* decreases at higher D. If there does exist a real, finite critical binding dimensionality with $D_c > 5$

FIG. 10. Dimensionality dependence of the ground-state-energy branch point λ^* for HEC, Chandrasekhar (C), and exact energies, as discussed in text. The exact curve represents only a possible curve passing through exact values of λ^* known at $D = 1$, 3, 5.

then it is possible that $\theta^* = 1$ at D_c, indicating a removal of the branch-point behavior. For $D < 3$ Fig. 9 suggests that there may be a dimensionality at which the exact $\theta^* = \frac{3}{2}$, corresponding to the same value obtained using finite parametrization in the trial wave functions. Such a value of D would be a logical point about which to perform a perturbation
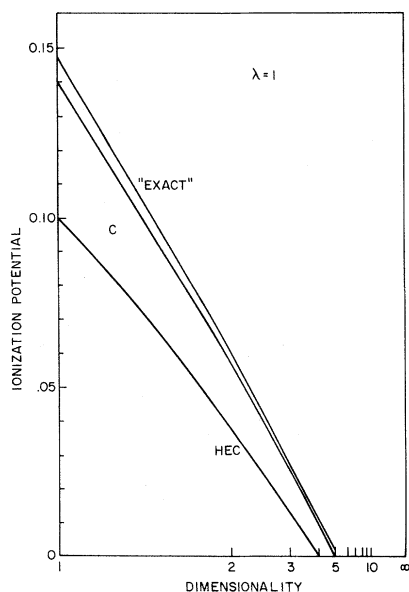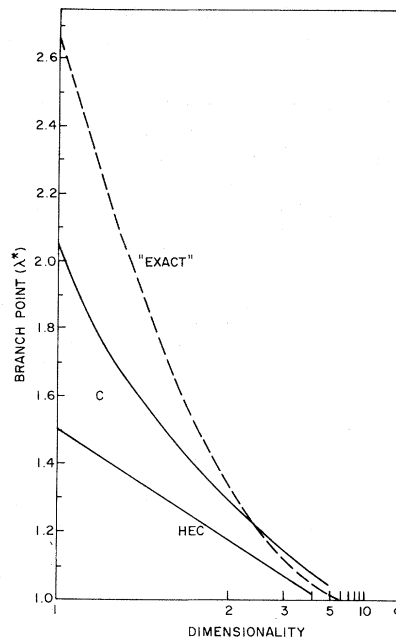

FIG. 9. Dimensionality dependence of the ground-state ionization potential of the hydride ion for the HEC, Chandrasekhar (C), and exact energies as discussed in the text. The "exact" curve represents a parabolic fit (IP $= -0.039602 + 0.209676 \, D^{-1} - 0.022849 \, D^{-2}$) to the accurately known energies at $D = 1$, 3, 5. Note that dimensionality units have been scaled to $1/D$.
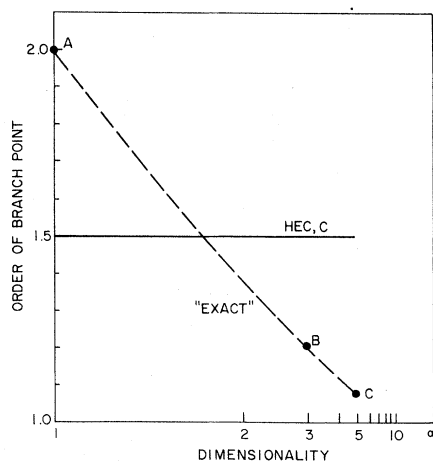

FIG. 11. Dimensionality dependence of the ground-state-energy branch-point singularity order θ^*, as discussed in text. The exact curve represents a possible curve through the known exact values at $D = 1$, 3, 5.

expansion for θ^*. Rosenthal concluded for δ-function model ($D=1$) that the energy has a pair of branch points in the complex λ plane at $|\lambda| \cong 2.9$ of the type $[(\lambda - z)(\lambda - \bar{z})]^m$, where z and $\bar{z}$ are complex conjugates and $m \cong 1.1$. However, we do not feel that these singularities need to be identified as the $D \to 1$ limit of our λ^* (having hypothetically fissioned into two branch points which move off the real axis). Instead it seems more plausible in terms of the present understanding of the continuum penetration phenomenon[6] that θ^* increases smoothly to 2 as D decreases to 1, to leave the simple parabolic tangency to the continuum edge noted by Rosenthal. It is entirely possible that the pair of singularities near $|\lambda| = 2.9$ exist for all $D > 1$; their effect on the corresponding perturbation coefficients would be relatively small compared to the effect of the real-axis singularity at λ^* closer to the origin.

While a knowledge of the exact λ dependence of ϵ_D at $D = 1, 3, 5$ has been useful for comparison with the HEC and Chandrasekhar results, it would be desirable to have accurate values of θ^*, ϵ_D, and λ^* over a continuous range of dimensionalities. A natural set of functions for such calculations is

the D-dimensional generalization of the Hylleraas coordinates.[1] A brief description of these coordinates and matrix elements is contained in Appendix B.

C. Comparison of λ-perturbation expansion coefficients for $D = 1, 3, 5$

In Table I we display the λ-perturbation energy coefficients for $D = 1$, 3, and 5 from Refs. 7 and 25. All energies have been converted to dimensionality-scaled atomic units. The coefficients are defined by

$$\epsilon_D(\lambda) = \sum_{k=0}^{} \lambda^k \epsilon_D^{(k)}, \qquad (47)$$

with $\epsilon_D^{(k)}$ being the kth-order energy coefficient.

Through second order the coefficients show a tendency to decrease binding as D increases. Commencing with $\epsilon_D^{(3)}$, however, the coefficients at higher D in general lead to *more* stability, in contrast to our simple arguments of Sec. VI A. The coefficients for $D = 1$ show the oscillations in sign resulting from the probable existence of a conjugate pair of branch points off the real λ axis.

We conclude this section by investigating further

TABLE I. Ground-state λ-perturbation energy coefficients $\epsilon_D^{(k)}$ in dimensionality-scaled atomic units.

k	$D = 1$[a]	$D = 3$[b]	$D = 5$[c]
0	-1.0	-1.0	-1.0
1	0.5	0.625	$0.656\,25$
2	$-0.162\,793\,409 \times 10^0$	$-0.157\,666\,428 \times 10^0$	$-0.157\,578\,718 \times 10^0$
3	$0.139\,891\,477 \times 10^{-1}$	$0.869\,902\,9 \times 10^{-2}$	$0.735\,983\,18 \times 10^{-2}$
4	$0.164\,276\,853 \times 10^{-2}$	$-0.888\,705 \times 10^{-3}$	$-0.136\,542\,90 \times 10^{-2}$
5	$0.170\,091\,337 \times 10^{-4}$	$-0.103\,6374 \times 10^{-2}$	$-0.135\,530\,80 \times 10^{-2}$
6	$-0.527\,475\,862 \times 10^{-4}$	$-0.612\,932 \times 10^{-3}$	$-0.925\,337\,2 \times 10^{-3}$
7	$-0.132\,910\,507 \times 10^{-4}$	$-0.372\,184 \times 10^{-3}$	$-0.659\,269\,2 \times 10^{-3}$
8	$-0.518\,533\,778 \times 10^{-6}$	$-0.242\,874 \times 10^{-3}$	$-0.492\,136\,2 \times 10^{-3}$
9	$0.669\,790\,439 \times 10^{-6}$	$-0.165\,662 \times 10^{-3}$	$-0.378\,761\,4 \times 10^{-3}$
10	$0.216\,734\,991 \times 10^{-6}$	$-0.116\,179 \times 10^{-3}$	$-0.298\,538\,8 \times 10^{-3}$
11	$0.129\,695\,081 \times 10^{-7}$	$-0.833\,02 \times 10^{-4}$	$-0.240\,162\,8 \times 10^{-3}$
12	$-0.125\,061\,648 \times 10^{-7}$	$-0.608\,81 \times 10^{-4}$	$-0.196\,600 \times 10^{-3}$
13	$-0.460\,944\,210 \times 10^{-8}$	$-0.452\,32 \times 10^{-4}$	$-0.163\,364 \times 10^{-3}$
14	$-0.330\,178\,625 \times 10^{-9}$	$-0.340\,80 \times 10^{-4}$	$-0.137\,494 \times 10^{-3}$
15	$0.287\,250\,960 \times 10^{-9}$	$-0.259\,93 \times 10^{-4}$	$-0.117\,024 \times 10^{-3}$
16	$0.113\,288\,498 \times 10^{-9}$	$-0.200\,34 \times 10^{-4}$	$-0.100\,572 \times 10^{-3}$
17	$0.861\,026\,942 \times 10^{-11}$	$-0.155\,86 \times 10^{-4}$	$-0.871\,84 \times 10^{-4}$
18	$-0.753\,861\,428 \times 10^{-11}$	$-0.122\,26 \times 10^{-4}$	$-0.761\,44 \times 10^{-4}$
19	$-0.305\,298\,953 \times 10^{-11}$	-0.9661×10^{-5}	$-0.669\,70 \times 10^{-4}$
20	$-0.226\,895\,585 \times 10^{-12}$	-0.7686×10^{-5}	$-0.592\,46 \times 10^{-4}$
21		-0.6152×10^{-5}	$-0.527\,30 \times 10^{-4}$

[a] From the δ function model, Ref. 7.
[b] Reference 25.
[c] From $2p^2\,{}^3P$ coefficients, Ref. 25.

the relative stability of the higher-order $D=5$ perturbation coefficients with respect to those at $D=3$. Analysis of the extensive perturbation expansions of Ref. 26 for the $1s^2\,^1S$ and $2p^2\,^3P$ states shows that these higher-order effects can be attributed almost entirely to the Coulomb repulsion operator $1/r_{12}$. For instance at $\lambda=0.5$ the average repulsion energies are 0.236 a.u. at $D=3$ and 0.251 a.u. at $D=5$. At $\lambda=1$, however, the relative magnitudes of repulsion energies are reversed: 0.311 a.u. at $D=3$ and 0.299 a.u. at $D=5$, indicating that the observed decrease in binding energy in going from $D=3$ to $D=5$ at $\lambda=1$ cannot be attributed to the average value of $1/r_{12}$. The most important factor leading to the reduction in binding energy at higher D values and large λ is the screening of the electrons from the attractive nuclear charge by the integration-volume element.

VII. CONCLUDING REMARKS

We have introduced dimensionality as a continuous parameter in the description of ground-state binding energies for the two-electron atom. Variational calculations with the HEC and Chandrasekhar wave functions showed a decrease in binding energy as dimensionality is increased. Each function leads to a prediction of a critical binding dimensionality D_c above which no binding is observed in the H^- negative ion. $D_c=3.99$ for HEC while angular correlation in the Chandrasekhar function gives $D_c=4.89$. Exact $D=1,3,5$ energies suggest $D_c=5.18$.

Equivalence of the $D=1$ and $D=5$ ground states to those of the δ-function model and the $2p^2\,^3P$ doubly excited state at $D=3$, respectively, was shown. Accurate binding energies as a continuous function of D are needed either to establish or disprove the existence of a finite critical binding dimensionality at $D>5$.

Until now the $2p^2\,^3P$ state $(D=3)$, the $1s^2\,^1S$ ground state $(D=3)$, and the δ-function model have been regarded as separate problems. By following a ground-state energy "trajectory" as a function of D, it is evident that these "physical" problems occur at the integer values $D=5$, 3, and 1. Similar trajectories for the branch point λ^* and the critical exponent θ^* will be invaluable for locating and classifying singularities. Just as the energy appears to be described by complex λ branch points at $D=1$, we do not find it unlikely that complex dimensionalities may eventually prove to be important in this problem.[27]

The notion that wave functions and energies of the $D=3$ ground state may eventually be obtained from an expansion about $D=1$ is very appealing. If this proves to be possible then similar use of

the δ-function model for many-electron atoms and molecules may well be justified.

APPENDIX A: EQUIVALENCE OF THE $D=5$ GROUND STATE AND THE $D=3$ $2p^2\,^3P$ STATE

In terms of the unscaled coordinates R_1, R_2, R_{12}, the D-dimensional Laplacian $\Delta_1^{(D)}+\Delta_2^{(D)}$ becomes

$$\Delta_D \equiv \frac{\partial^2}{\partial R_1^2}+\frac{\partial^2}{\partial R_2^2}+\frac{2\partial^2}{\partial R_{12}^2}+\frac{R_{12}^2+R_1^2-R_2^2}{R_1 R_{12}}\frac{\partial^2}{\partial R_1 \partial R_{12}}$$
$$+\frac{R_{12}^2+R_2^2-R_1^2}{R_2 R_{12}}\frac{\partial^2}{\partial R_2 \partial R_{12}}$$
$$+(D-1)\left(\frac{1}{R_1}\frac{\partial}{\partial R_1}+\frac{1}{R_2}\frac{\partial}{\partial R_2}+\frac{2}{R_{12}}\frac{\partial}{\partial R_{12}}\right).$$

$$(A1)$$

We define the function $P=X_1 Y_2 - Y_1 X_2$, where X_i and Y_i are any two different Cartesian coordinates for electron i. If χ is a function dependent upon only the coordinates R_1, R_2, and R_{12}, then in D dimensions

$$(\Delta_1^{(D)}+\Delta_2^{(D)})P\chi=\left[P(\Delta_1^{(D)}+\Delta_2^{(D)})+2\left(Y_2\frac{\partial}{\partial X_1}-X_2\frac{\partial}{\partial Y_1}\right.\right.$$
$$\left.\left.-Y_1\frac{\partial}{\partial X_2}+X_1\frac{\partial}{\partial Y_2}\right)\right]\chi$$
$$=P\left(\Delta_D+\frac{2}{R_1}\frac{\partial}{\partial R_1}+\frac{2}{R_2}\frac{\partial}{\partial R_2}+\frac{4}{R_{12}}\frac{\partial}{\partial R_{12}}\right)\chi$$
$$=P(\Delta_{D+2}\chi).\qquad(A2)$$

Since the potential energy commutes with P, we have the result that if χ is an eigenfunction of the $(D+2)$-dimensional Hamiltonian

$$-\tfrac{1}{2}\Delta_{D+2}-\frac{1}{R_1}-\frac{1}{R_2}+\frac{\lambda}{R_{12}},$$

then $P\chi$ is necessarily an eigenfunction of the Hamiltonian in D dimensions. In particular, if χ is the exact ground-state wave function in five dimensions, then $P\chi$ is an eigenfunction (of the same energy) with one unit of angular momentum in three dimensions. This must be the $2p^2\,^3P$ state since χ is nodeless. Identical correspondences also exist for the excited bound and continuous states as well.

It can be shown in addition that the average energy of *any* $D=5$ trial wave function of the type $\varphi(R_1,R_2)$ is equal to that of the trial wave function $P\varphi(R_1,R_2)$ when $D=3$. For instance our HEC results for $D=5$ are identical to those reported by Stillinger and Stillinger[5] for the $D=3$ $2p^2\,^3P$ state.

APPENDIX B: D-DIMENSIONAL HYLLERAAS COORDINATES

In direct analogy to the Hylleraas coordinates for $D=3$, we define

$$u = r_{12}, \quad s = r_2 + r_1, \quad t = r_2 - r_1. \tag{B1}$$

The ground-state wave function can be expanded in terms of the functions $e^{-ks/2}s^l u^m t^n$, where k may be regarded as a scale factor. The volume element in this space is (to within a constant which can be ignored)

$$d\tau = u(s^2 - t^2)[(s^2 - u^2)(u^2 - t^2)]^{(D-3)/2} \, ds \, du \, dt, \tag{B2}$$

and thus all energy matrix elements for the ground-state energy can be expressed in terms of the integral

$$B_D(k, p, q, r) = \int_0^\infty ds \int_0^s du \int_0^u dt \, e^{-ks} s^p u^q t^r [(s^2 - u^2)(u^2 - t^2)]^{(D-3)/2} \tag{B3}$$

$$= \frac{\Gamma(a)}{4k^a} B\left(\frac{q+r+D-1}{2}, \frac{D-1}{2}\right) B\left(\frac{r+1}{2}, \frac{D-1}{2}\right), \tag{B4}$$

where $a = p + q + r + 2D - 3$ and $B(m, n) = \Gamma(m)\Gamma(n)/\Gamma(m+n)$ is the beta function.

[1] E. A. Hylleraas, Z. Phys. 54, 347 (1929).

[2] C. Eckart, Phys. Rev. 36, 878 (1930).

[3] S. Chandrasekhar, Astrophys. J. 100, 176 (1944).

[4] F. H. Stillinger, J. Chem. Phys. 45, 3623 (1966).

[5] F. H. Stillinger and D. K. Stillinger, Phys. Rev. A 10, 1109 (1974).

[6] F. H. Stillinger and T. A. Weber, Phys. Rev. A 10, 1122 (1974).

[7] C. M. Rosenthal, J. Chem. Phys. 55, 2474 (1971).

[8] (a) K. G. Wilson and M. E. Fisher, Phys. Rev. Lett. 28, 240 (1972); (b) K. G. Wilson, Phys. Rev. Lett. 28, 548 (1972).

[9] A. Bottino, A. M. Longoni, and T. Regge, Nuovo Cimento 23, 954 (1962).

[10] S. C. Frautschi, Regge Poles and S-Matrix Theory (Benjamin, New York, 1963).

[11] For a pertinent description of the spherical functions see D. R. Herrick and O. Sinanoğlu, Rev. Mex. Fis. 22, 1 (1973).

[12] Handbook of Mathematical Functions, NBS Appl. Math. Ser. No. 55, edited by M. Abramowitz and I. Stegun (U. S. GPO, Washington, D. C., 1964).

[13] S. P. Alliluev, Zh. Eksp. Teor. Fiz. 33, 200 (1957) [Sov. Phys.—JETP 6, 156 (1958)].

[14] V. Fock, Z. Phys. 98, 145 (1935).

[15] An interesting consequence of this "dimensionality barrier" is that S-wave shape resonances may occur in electron-hydrogen scattering for $D > 3$.

[16] D. R. Herrick, J. Math. Phys. (to be published).

[17] We retain here the $D = 3$ convention that states with $\Lambda = 0, 1, 2, \ldots$ are labeled, respectively, $s, p, d, \ldots$

[18] (a) A. A. Frost, J. Chem. Phys. 25, 1150 (1956); (b) A. A. Frost and F. E. Leland, J. Chem. Phys. 25, 1154 (1956).

[19] R. J. White and F. H. Stillinger, J. Chem. Phys. 52, 5800 (1970).

[20] R. A. Bonham and D. A. Kohl, J. Chem. Phys. 45, 2471 (1966).

[21] Described in Ref. 6.

[22] Chandrasekhar energies are very insensitive to γ for $D > 7$, but analytic minimization leads to a quartic polynomial in γ for each value of η.

[23] T. Kato, Trans. Am. Math. Soc. 70, 195 (1951).

[24] C. L. Pekeris, Phys. Rev. 126, 1470 (1962).

[25] J. Midtdal, Phys. Rev. 138, A1010 (1965).

[26] K. Aashamar, Phys. Math. Univ. Oslo. Inst. Rep. No. 35, 36 (1969).

[27] Complex dimensionalities in one sense are familiar to the group theorist. Consider, for example, the conjugate dimensionalities $D = 3 \pm i$ defined by the coordinates $(x, y, z, \pm it)$. Transformations which leave invariant $x^2 + y^2 + z^2 - t^2$ define the noncompact group $O(3, 1)$.